AUTHIGENIC K-NH_4-FELDSPAR IN SANDSTONES: A FINGERPRINT OF THE DIAGENESIS OF ORGANIC MATTER

KARL RAMSEYER[1], LARRYN W. DIAMOND[2], AND JAMES R. BOLES[3]
[1] *Geologisches Institut, Universität Bern, Baltzerstrasse 1, CH-3012 Bern, Switzerland*
[2] *Mineralogisch-Petrographisches Institut, Universität Bern, Baltzerstrasse 1, CH-3012 Bern, Switzerland*
[3] *Department of Geological Sciences, University of California, Santa Barbara, California 93117 USA*

ABSTRACT: **In arkosic sandstones of the San Joaquin and Los Angeles Basins presently at temperatures between 35°C and 174°C, trace amounts of authigenic K-NH_4-feldspar are present as microfracture fillings and overgrowths on detrital K-feldspar. Microchemical analyses of this authigenic phase reveal up to 80 mole % buddingtonite. The largest ammonium concentrations are observed in a sandy interval of the Antelope shale (80 mole %) and in the Stevens Sands (≈ 50 mole %) of the San Joaquin Basin. This latter unit was deposited as a turbidite in the organic-rich Fruitvale Shale, an equivalent of the Antelope Shale. The lowest ammonium contents (0-16 mole %) are present in the shallow-marine Vedder Sands and the marginal marine San Joaquin Formation in the same basin.**

Petrographic, $\delta^{18}O$, $\delta^{13}C$, and $^{87}Sr/^{86}Sr$ analyses of a dolomite cement that postdates authigenic K-NH_4-feldspar indicate that the feldspar precipitated below 28°C in the zone of methanogenesis, from pore waters with the same Sr signature as sea water at the time of sedimentation. Authigenic K-NH_4-feldspar is thus an early-diagenetic phase that crystallized prior to oil migration, under anoxic conditions when organic matter releases ammonium.

The source of ammonium is bacterial decay of organic matter in the sandstones themselves and/or in contemporaneous shales.

INTRODUCTION

Over the past few years a number of studies have focused on the sources and sinks of nitrogen in sediments (Gulbrandsen 1974; Loughnan et al. 1983; Krumbein 1983; Jenden et al. 1988; Daniels and Altaner 1990; Compton et al. 1992; Williams et al. 1992). Nitrogen derives dominantly from organic matter and its decay products, although in some cases (e.g., Jenden et al. 1988) input from basement metamorphic rocks may also be important. Owing to the different possible redox states of nitrogen, i.e., NO_3^-, N_2, NH_4^+ (Froelich et al. 1979; Krumbein 1983), sinks are more diverse. During degradation of organic matter nitrogen is liberated in a variety of species: as nitrate in the aerobic zone, as nitrogen gas in the manganese and nitrate reduction zones, and as ammonium in the anoxic environments of iron and sulfate reduction, methane formation, and thermal decarboxylation (Curtis 1978; Froelich et al. 1979). Both nitrate and nitrogen gas probably diffuse out of sediments into the overlying open water, whereas ammonium generated at greater depth may remain trapped in interstitial water or diffuse into the oxic zone higher up (Froelich et al. 1979). During diagenesis this released ammonium can be incorporated into authigenic silicates such as feldspars, micas, or zeolites, in crystallographic sites normally occupied by alkali ions (Hallam and Eugster 1976).

In the case of early diagenetic precipitation, the concentration of incorporated ammonium may depend in part on the original concentration of detrital organic matter in the sandstone and on the proximity and amount of organic matter in associated shales. During intermediate-burial diagenesis, in contrast, an external source, such as oil generation in adjacent mudrocks, is a more probable origin of ammonium in sandstones (Ferrell and Williams 1991; Williams et al. 1992). Incorporation of ammonium into authigenic minerals during intermediate burial diagenesis is well documented for illite in both sandstones and organic-rich mudrocks (e.g., Williams et al. 1989; Ferrell and Williams 1991, Compton et al. 1992; Williams et al. 1992), but so far no example has been published of an early diagenetic origin for an ammonium-bearing authigenic mineral.

The aims of this paper are (1) to report occurrences of early diagenetic K-NH_4-feldspar, (2) to quantify the composition of K-NH_4-feldspar, (3) to determine the timing of K-NH_4-feldspar precipitation, and (4) to explore the origin of ammonium.

The samples for this study were taken from well cores situated along the published W-E cross section of the southern San Joaquin Basin (Fig. 1, Table 1; California Division of Oil and Gas, Bakersfield, CA, 1982). Present-day burial temperatures at the sample positions range between 35°C and 174°C, according to shut-in well temperatures and calculated values from the AAPG Geothermal Gradient Map No. 22 (1974). These temperatures are maximum values except for the uplifted regions on the west side of the basin (Fig. 1).

Also included in this study is a set of carbonate-cemented sandstones where authigenic K-NH_4-feldspar is present as microfracture filling in detrital K-feldspar (Tab. 1). The pore-filling carbonate cement forms zones 1.5 m thick randomly distributed in the porous sandstone succession (Boles and Ramseyer, 1987). Stable-isotope analyses of individual carbonate zones indicate cementation temperatures between 28°C and 93°C (Table 2; Boles and Ramseyer 1987; Schultz et al 1989; Wood and Boles 1990). Samples from these cement zones have been used to determine the thermal onset of authigenic K-NH_4-feldspar crystallization.

For comparative purposes, two sandstone samples from the Los Angeles Basin (provided by R. Coffman, UCSB) have also been added to the suite for investigation.

GEOLOGIC SETTING

The southern San Joaquin Basin is the southernmost part of the Great Valley of California, and is situated between the Sierra Nevada batholith to the east and the Coast Ranges with the presently active San Andreas fault system to the west (Fig. 1). In its deepest part the basin contains more than 8000 m of Tertiary siliciclastic sediments (Bartow and McDougall 1984). The central and eastern region of the southern San Joaquin Basin is characterized by a single burial cycle with no major uplift but with widely varying burial rates (Callaway 1971; Bent 1985; Graham and Williams 1985). For the western part of the basin a complex history of burial and uplift during Tertiary times is typical. Tectonic activity is restricted to normal faulting on the eastern side of the basin and along the White Wolf Fault in the south, and to the large area of uplift along the San Andreas Fault system (Fig. 1).

The Tertiary sedimentary cycle starts in the eastern and central part of the basin with Eocene continental conglomerates and sandstones overlapping crystalline basement, whereas in the western part Paleocene marine sediments transgress Upper Cretaceous marine deposits (Moxon 1988).

The marine incursion in the central and eastern part during Eocene time led to the deposition of shallow-marine, fine- to medium-grained sands of Eocene and Oligocene age. During Miocene times, subsidence continued and deeper-marine siltstones, sandy and organic-rich shales, and turbidites were deposited in the basin center while on the eastern margin, shallow-marine and terrestrial sandstones were deposited. The drop in eustatic sea

JOURNAL OF SEDIMENTARY PETROLOGY, VOL. 63, NO. 6, NOVEMBER, 1993, P. 1092–1099
 0022-4472/93/0063-1092/$03.00

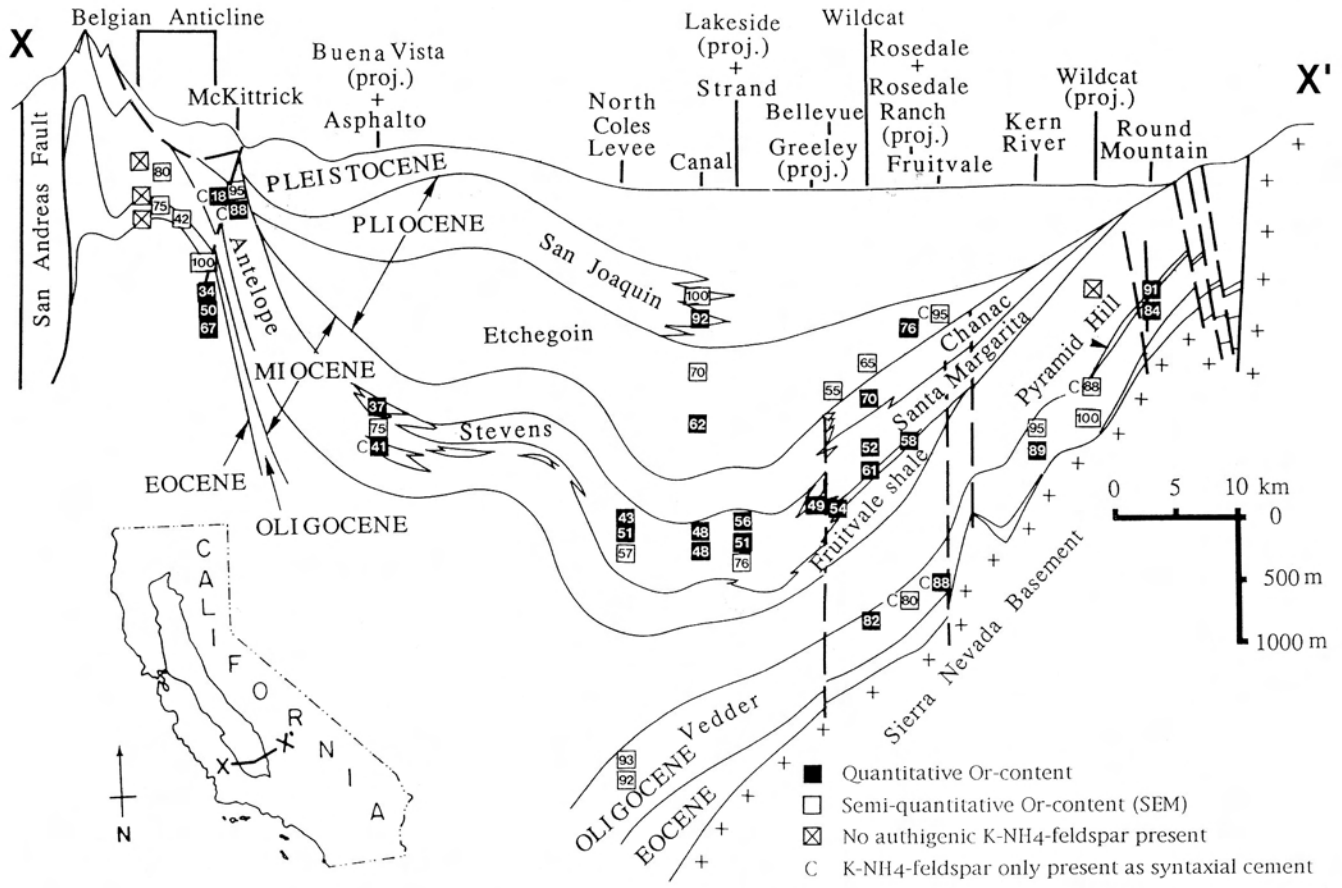

FIG. 1.—Cross section through the southern San Joaquin Basin with the most important lithostratigraphic units, oil fields, and sample locations (after California Oil and Gas Fields, 1982, a publication of California Division of Oil and Gas, Bakersfield, Calif.).

level during latest Miocene times (Haq et al. 1987), as indicated by the basinwide regression, changed the depositional environment from marine to terrestrial. Sandstones and conglomerates were deposited throughout the southern San Joaquin Basin from Late Miocene time onwards (Bartow and McDougall 1984).

ANALYTICAL METHODS

Cathodoluminescence, optical petrography, backscattered electron imaging, and electron microscopy were applied to detect and quantify the chemical composition of authigenic K-NH_4-feldspars.

In a first step, a high-sensitivity cathodoluminescence microscope (Ramseyer et al. 1989) was used to search for nonluminescent authigenic feldspar (Kastner and Siever 1979; Marshall 1988) present as syntaxial overgrowths or microfracture fillings in bluish-luminescing detrital K-feldspar grains (Fig. 2B, E, H). Polished thin sections coated with aluminum were bombarded with a 30 keV electron beam at a current density of 0.3 $\mu A/mm^2$. Color slides of the luminescence features were taken with Ektachrome 400 color transparency film and developed at 800 ASA.

Detrital K-feldspar grains with nonluminescing zones were then observed with a CAMSCAN S4 scanning electron microscope (SEM) in backscattered mode to differentiate between pure K-feldspar and K-NH_4-feldspar. Because no alkali ions other than K^+ are present, differentiation is straightforward. Uptake of NH_4^+ into K-feldspar decreases the mean atomic number of the mineral and therefore decreases the intensity of its backscattered signal (Figs. 2C, F, I). Semiquantitative analyses of the authigenic K-NH_4-feldspar were obtained with a Tracor Northern TN5500 energy-dispersive spectrometer (EDS) mounted on the SEM.

Quantitative analyses were performed at the previously selected areas with a CAMECA SX50 electron microprobe equipped with 4 WDS spectrometers, a Princeton Gamma Tech EDS system, and an anticontamination attachment consisting of vacuum cold traps and an oxygen jet. To minimize absorptive loss of N $K\alpha$ X-ray emission, the aluminum coating was removed from the polished thin sections already analyzed by cathodoluminescence and SEM-EDS, and the sections were then recoated with a thin film of carbon ($\approx$ 120 Å). The areas for analysis were also encircled with silver paint to ensure good electrical conductivity.

Tests were conducted to optimize the instrumental operating conditions such that high X-ray count rates were obtained with minimal surface damage by the electron beam. As a result, final analyses were performed with a beam energy of 10 keV, a beam current of 10 nA, and a tightly focused beam rastered over an area of 2.2 × 4.8 μm (25000× magnification). K, Ca, and Ba were measured with a PET crystal, Na, Al and Si with a TAP crystal, and N with an OVONYX® OV-060A W/Si multilayer reflector (Ovonic Synthetic Materials Co., Inc.) characterized by an interlayer 2d spacing of approximately 61 Å. Conventional gas-flow proportional X-ray detectors were used with a P-10 gas mixture (90% Ar, 10% CH_4). Because the N $K\alpha$ emission line is well defined and free of any spectral interferences in the natural and standard materials examined, N intensities were acquired by the conventional peak-minus-background method, in which the background intensity below the peak was estimated as the mean of the background signals at offsets of 2.4 Å (0.04000 sinθ) above and below the peak position.

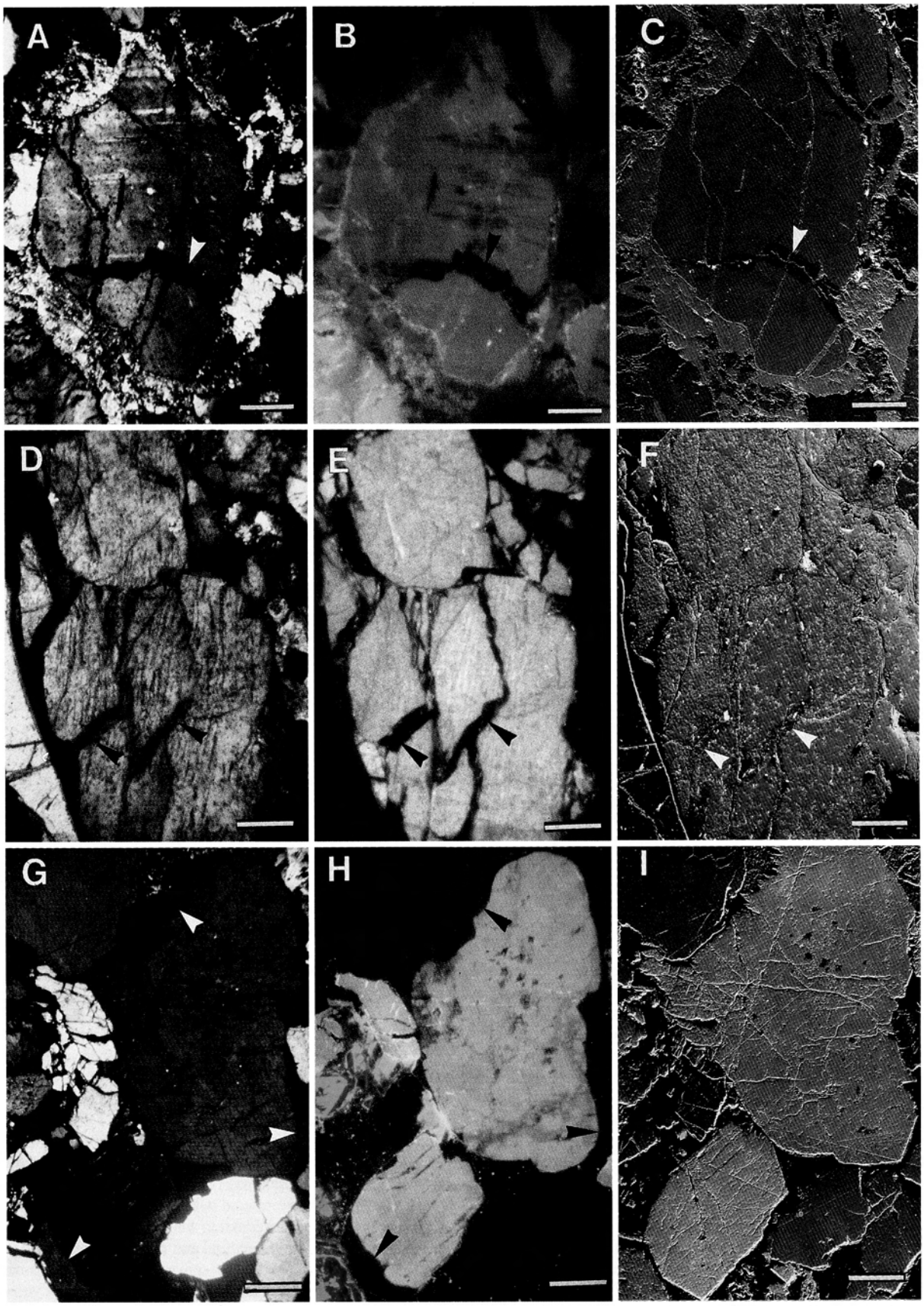
A
B
C
D
E
F
G
H
I

TABLE 1.—*Sample locations, present-day subsurface temperature, occurrence, and chemical composition of authigenic K-NH_4-feldspar*

Basin	Oil Field	Well	Stratigraphic Unit	Depth (m)	Temp. (°C)@	Occurrence		Chemical Composition					Or # (EDS)
						Fracture	Cement	Or	Budd	Ab	An	Cel	
San Joaquin	Round Mountain (ROMO)	USL #101	Pyramid Hill	568.5	35	x		90.8	9.0	0.1	0.0	0.0	85
							x	94.0	5.6	0.1	0.3	0.0	85
			Vedder	584.0	36	x		84.1	15.9	0.0	0.0	0.0	75
							x	94.4	5.3	0.0	0.0	0.3	92
	Kern River (KERI)	Soverign WD-1	Eocene	1764.8	73	x		89.0	9.0	0.4	0.0	1.6	95
	Fruitvale (FRU)	Shellabargar Sheldon #1	Vedder	3028.2	99		x	98.1	0.0	1.1	0.8	0.0	100
							x	88.2	9.6	1.0	1.0	0.2	86
	Rosedale Ranch (RORA)	Texaco CWL #1	Etchegoin	1046.7	45	x		76.1	23.8	0.1	0.0	0.0	80
	Wildcat (WC)	Ohio KCL G-1	Chanac	1589.5	60	x		69.5	29.5	0.4	0.0	0.6	75
							x	74.7	23.7	0.0	1.1	0.5	80
			St. Margarita	1957.1	70	x		52.1	47.9	0.0	0.0	0.0	50
							x	63.2	35.9	0.6	0.3	0.0	50
			Stevens	2225.0	78	x		61.0	38.0	0.5	0.5	0.0	72
			Vedder	3211.1	104	x		82.4	15.8	1.5	0.3	0.0	88
	Rosedale (ROS)	Humble Stevens #4	Stevens	2201.3	77	x		57.6	41.2	0.7	0.0	0.5	55
	Bellevue (BEL)	Superior KCL #9	Stevens	2194.0	77	x		53.6	45.2	1.2	0.0	0.0	50
	Greeley (GRE)	St. Wegis Commission #1	Stevens	2368.9	81	x		49.0	50.5	0.3	0.2	0.0	50
	Strand (STR)	KCL 36-7	Stevens	2473.5	90	x		56.4	42.7	0.7	0.0	0.2	50
	Lakeside (LAK)	Tidewater KCL 36-35	Stevens	2573.2	103	x		51.1	47.7	1.2	0.0	0.0	48
	Canal (CAN)	Canal KCL A-21	San Joaquin	1129.3	52	x		91.9	3.6	1.9	0.5	2.1	100
			Etchegoin	1759.6	71	x		62.7	36.8	0.5	0.0	0.0	70
		KCL E-23	Stevens	2472.5	93	x		47.8	51.0	0.4	0.0	0.8	45
	North Coles Levee (NCL)	Richfield A-52	Stevens	2603.0	102+	x		43.2	53.9	1.3	0.8	0.8	40
		NCL 487-29	Stevens	2737.4	88*	x		44.7	54.8	0.5	0.0	0.0	47
		NCL 488-29	Stevens	2629.3	43*	x		51.0	47.3	0.6	0.8	0.3	45
			Stevens	2632.5	75*	x		43.1	55.3	0.4	0.0	1.2	55
			Stevens	2727.4	28*	x		45.7	53.5	0.6	0.0	0.2	55
			Stevens	2750.5	57*	x		48.9	47.6	1.0	0.5	2.0	54
	Asphalto (ASP)	Roco NPR #352	Stevens	1751.1	73	x		36.9	62.2	0.7	0.7	0.0	36
							x	43.1	56.5	0.4	0.0	0.0	42
	Buena Vista (BUVI)	Ohio KCL A-8	Stevens	3063.8	114		x	41.2	57.6	0.9	0.3	0.0	45
	McKittrick (McK)	Getty Shamrock 87A	Stevens	870.2	>45	x		88.5	6.0	2.1	0.3	3.1	100
	Belgian Anticline Main Area (BAMA)	Midway McKittrick #1	Antelope	1119.5	>52		x	17.9	80.5	0.5	0.8	0.3	20
			Eocene	1736.4	>72	x		34.4	63.5	0.9	0.0	1.3	30
							x	60.7	38.8	0.0	0.5	0.0	55
			Eocene	1804.4	>74	x		50.8	48.0	0.0	0.9	0.3	55
							x	48.9	50.2	0.4	0.0	0.5	48
			Eocene	1922.1	>78	x		67.2	30.7	0.5	1.1	0.5	70
Los Angeles	Santa Fe Springs	Union Fairwell 18	Upper Miocene	2927.3	120–127	x		49.5	48.7	0.8	0.0	1.0	48
		Santa Fe Springs 143-B	Upper Miocene	2596.9	110–115	x		48.6	50.6	0.5	0,3	0.0	45
							x	52.4	42.6	0.9	1.8	2.3	47

@ Present-day subsurface temperature was calculated from the AAPG Geothermal Gradient Map No. 22 (1974) except where shut-in well values (denoted by cross) exist or where carbonate-cemented samples with $\delta^{18}O$-derived crystallization temperatures (denoted by asterisk) exist. Temperatures for uplifted areas on the west side of the San Joaquin Basin are minimum values.

Semiquantitatively determined orthoclase content of authigenic K-NH_4-feldspar in mole %, based on SEM-EDS analyses.

←

FIG. 2.—Photomicrographs of authigenic K-NH_4-feldspar from the San Joaquin Basin. **A)** Crossed-polarized transmitted-light view of a detrital K-feldspar grain with a fracture filling (arrow) of low birefringence, from the Stevens Sand (2750.5 m), North Coles Levee oil field, California. Note that the fracture formed during burial compaction of the unconsolidated sand but prior to the surrounding calcite cement which, according to $\delta^{18}O$ stable-isotope data, precipitated at 57°C (Boles and Ramseyer 1987). Scale bar = 100 μm. **B)** Cathodoluminescence photograph of the same field of view as in Fig. 2A. Note that the fracture-filling authigenic K-NH_4-feldspar is nonluminescent (arrow), whereas the detrital grain shows a blue luminescence. Note also that both sides of the fracture are irregular but match together. Scale bar = 100 μm. **C)** Backscattered electron image of the same field of view as in Fig. 2B. Note that the fracture-filling authigenic K-NH_4-feldspar (arrow) has a lower intensity than the host detrital K-feldspar due to its lower mean atomic number. Scale bar = 100 μm. **D)** Crossed-polarized transmitted light view of a detrital K-feldspar grain with a network of low-birefringence fracture fillings (arrow), Stevens Sand (2194.0 m), Bellevue oil field, California. Scale bar = 100 μm. **E)** Cathodoluminescence photograph of the same field of view as in Fig. 2D. Note the complex fracture pattern (arrow). Scale bar = 100 μm. **F)** Backscattered electron image of the same field of view as in Fig. 2E. Note the lower intensity of the BSE signal in the network of fractures with authigenic K-NH_4-feldspar (arrow) in comparison to the detrital K-feldspar grain. Scale bar = 100 μm. **G)** Crossed-polarized transmitted-light view of two detrital K-feldspar grains with authigenic syntaxial cement (arrow) showing a slightly different birefringence, Vedder Sand (3028.2 m), Fruitvale oil field, California. Scale bar = 200 μm. **H)** Cathodoluminescence photograph of the same field of view as in Fig. 2G. Note that the authigenic K-NH_4-feldspar overgrowths are nonluminescent (arrow), whereas the detrital grains show a bluish luminescence. Scale bar = 200 μm. **I)** Backscattered electron image of the same field of view as in Fig. 2H. Note that the authigenic K-NH_4-feldspar overgrowths are indistinguishable from the detrital K-feldspar. Scale bar = 200 μm.

TABLE 2.—*Isotopic signatures, volume data, and calculated precipitation temperatures of individual cement zones: ranges are given for dolomite, early calcite (shallow burial), and late calcite (intermediate burial) cements*

Well	Depth (m)	Cement		$\delta^{18}O$[1]	$\delta^{13}C_{PDB}$	$^{87}Sr/^{86}Sr$	Crystallization Temperature[2]
		Type	Vol%				
NCL 488–29	2727.4	Dolomite	40*	−0.4*	+9.0*	0.70865°	28
NCL 488–29	2629.3	Calcite	36	−5.5°	−10.4″	0.70825°	43
NCL 488–29	2750.5	Calcite	25	−6.8°	−7.7″	0.70825°	57
NCL 488–29	2632.5	Calcite	24	−8.2°	−3.6″	0.70805°	75
NCL 487–29	2737.4	Calcite	16°	−9.3°	−1.4″	0.70736°	88
NCL 12–31	2746.2	Present pore water				0.70721°	
NCL 14–31	2641.1	Present pore water		+2.8*			
KCLB 67–4	2750.0	Benthic foraminifera[3]				0.70863°	
		Dolomite	40–32°	−0.4/−2.5*	+9.0/+5.7*	0.70865° 0.70860°	28–41
		Early calcite	32–23°	−5.5/−8.1*	−4.3/−10.4″	0.70825° 0.70785°	43–74
		Late calcite	24–14°	−8.2/−9.8*	−3.6/−1.4″	0.70771° 0.70715°	75–93

* Data from Boles and Ramseyer (1987).
° Data from Schultz et al. (1989).
″ Data from Wood and Boles (1990).
[1] $\delta^{18}O$ values are quoted in the PDB scale except for the water analysis (NCL 12-31, 2746.2m; NCL 14-31, 2641.1m) where the SMOW scale is used.
[2] Crystallization temperatures of calcites and dolomites have been calculated from cement $\delta^{18}O$ values and pore water oxygen compositions. For dolomite a zero pore water $\delta^{18}O_{SMOW}$ value and for calcite a linear change of the pore water $\delta^{18}O_{SMOW}$ value from an initial marine signature (= 0) to the present day value of +2.8 was taken. The following fractionation equations were used: Calcite-water: $\delta^{18}O_{Cc} - \delta^{18}O_{H_2O} = 2.78^* (10^6/T^2) - 2.89$ (Friedman and O'Neil 1977). Dolomite-water: $\delta^{18}O_{Dol} - \delta^{18}O_{H_2O} = 2.78^* (10^6/T^2) + 0.11$ (Fritz and Smith 1970), where T is temperature in Kelvin.
[3] This benthic foraminifera was used to determine the seawater $^{87}Sr/^{86}Sr$ ratio during deposition of the Stevens Sand in late Miocene time.

Peak and background acquisition times were 10 s and 5 s, respectively, for Si, Al, Na, K, Ca, and Ba, whereas N was measured for 100 s on the peak and 50 s on each of the background positions. The standards used for signal calibration were orthoclase (Si and Al), adularia (K), albite (Na), hyalophane (Ba), synthetic anorthite (Ca), and a N-doped synthetic cordierite (Armbruster 1985). No peak shifts were noted between the standards and the natural samples analyzed, and full anticontamination procedures were used during both calibration and analysis.

Only analytical totals of 100 ± 2 wt % were accepted after stoichiometric addition of O and H and correction for the effects of absorption, fluorescence, and atomic number using the PAP algorithm (Pouchou and Pichoir 1984). Under these analytical conditions the detection limit for N, calculated from the 3σ value of the X-ray intensity at the N spectral position in a natural, N-free adularia, was found to be 0.3 wt % $(NH_4)_2O$ or approximately 3 mole % buddingtonite component ($NH_4AlSi_3O_8$).

TABLE 3.—*Electron microprobe analyses of authigenic K-NH_4-feldspar, expressed in wt % and mole % of the orthoclase, buddingtonite, albite, anorthite, and celsian endmember. The sample numbers represent the abbreviated oil field name and the depth of the sample shown in Table 1*

Sample	ROMO 584.0	KERI 1764.8	ROMO 584.0	WC 1589.5	McK 1736.4	NCL 2727.4	BAMA 1736.5	BAMA 1119.5
K_2O	15.69	15.04	13.31	12.57	11.73	7.58	6.39	3.01
$(NH_4)_2O$	0.49	0.85	1.39	2.20	2.97	4.91	6.52	7.48
Na_2O	0.00	0.05	0.00	0.12	0.10	0.06	0.11	0.06
CaO	0.00	0.00	0.01	0.00	0.06	0.00	0.00	0.08
BaO	0.07	0.40	0.00	0.12	0.16	0.07	0.40	0.10
Al_2O_3	18.42	18.10	18.39	18.61	18.75	19.12	19.21	19.47
SiO_2	65.91	65.53	66.72	67.81	67.61	69.12	68.80	68.64
Sum	100.58	99.97	99.82	101.43	101.37	100.86	101.43	98.84
Or	94.4	89.0	84.1	74.7	67.2	45.7	34.4	17.9
Budd	5.3	9.0	15.9	23.7	30.7	53.5	63.5	80.5
Ab	0.0	0.4	0.0	0.0	0.5	0.6	0.9	0.5
An	0.0	0.0	0.0	1.1	1.1	0.0	0.0	0.8
Cel	0.3	1.6	0.0	0.5	0.5	0.2	1.2	0.3
Si/Al[1]	3.01	3.07	3.08	3.09	3.06	3.07	3.04	2.99

[1] Si/Al is the atomic ratio of silica to aluminum.

OCCURRENCE OF AUTHIGENIC K-NH_4-FELDSPAR

Authigenic K-NH_4-feldspar is present in more than 80% of the 90 subsurface sandstone samples collected along a cross section through the southern San Joaquin Basin (Fig. 1, Table 1). Its occurrence may often be overlooked, because it crystallizes preferentially, i.e., in more than 80% of the observed cases, within brittle microfractures in K-feldspar grains (Fig. 2). As in albitization, microfracturing of such detrital K-feldspar grains is the result of mechanical compaction (Ramseyer et al. 1992). Authigenic syntaxial overgrowths on detrital K-feldspar grains are rare and well developed only in the Oligocene Vedder Sand on the eastern flank of the basin (Figs. 1, 2). The preference of authigenic K-NH_4-feldspar to precipitate in fractures may be the result of differences in the free energy of nucleation between narrow cracks and grain surfaces. In other words, the degree of oversaturation in the pore fluid needed to form stable K-feldspar nuclei is lower in narrow fractures or at grain contacts than on grain surfaces exposed to a pore space (Berner 1980). Other explanations, such as poisoning of the detrital grain surface by absorption of inorganic or organic substances, or the existence of a silica-rich dissolution surface, are unlikely since the depositional environment (except for the few nonmarine samples) and the origin of the detrital K-feldspar grains (first-cycle origin) are similar for the Vedder and Stevens Sands on the eastern side of the San Joaquin Basin (Webb 1981; Bartow and McDougall 1984; Boles and Ramseyer 1986).

Whether as microfracture fillings or as overgrowth cement, authigenic K-NH_4-feldspar is always in optical continuity with its host detrital grain. However, it often displays a slightly different birefringence due to compositional differences with respect to its host (Fig. 2A, D, G). The amount of authigenic K-NH_4-feldspar in a given sample depends primarily on the quantity of fractured detrital K-feldspar grains present. In general, since on a thin-section scale only a few grains are fractured, authigenic K-NH_4-feldspar is a trace phase.

CHEMICAL COMPOSITION OF K-NH_4-FELDSPAR

Quantitative microprobe analyses were carried out on a total of 32 samples from the southern San Joaquin Basin and the Los Angeles Basin. All these samples contain authigenic K-NH_4-feldspar as fracture fillings and/or as overgrowth cement (Table 1). Typical chemical compositions of authigenic K-NH_4-feldspar are shown in Table 3. The major constituents detected in the authigenic K-NH_4-feldspar are K, Al, Si, and N. Trace concentrations of Na, Ca, and Ba are sporadically present (Tables 1, 3). In addition, the chemical analyses reveal that the authigenic phase has a stoichiometric feldspar composition with a slightly higher concentration of Si than normal K-feldspar or buddingtonite (Table 3). Tests of the stability of the authigenic K-NH_4-feldspar phase under the electron beam showed that the apparent concentration of K decreases with continued electron bombardment, due to diffusive loss of matter from the bombarded volume of the sample. As a consequence, the apparent concentration of Si increases simultaneously by default. This apparent increase in Si concentration was found to be more pronounced in NH_4^+-rich feldspar than in K-rich feldspar. The high Si concentrations that appear in Table 3, indicated by Si/Al ratios in excess of 3, are therefore probably artifacts of the measurement technique and hence do not represent a real surplus of Si.

In the 32 samples analyzed quantitatively, the concentration of N varies between the detection limit, i.e., < 3 mole %, and 80.5 mole % buddingtonite component (Table 1). Similarly, the K concentrations of the 90 samples analyzed semiquantitatively by SEM-EDS imply a wide variability in the K/NH_4 ratio (Fig. 1). Note, however, that the SEM-EDS analyses differ from the quantitative electron microprobe analyses by up to 10 mole % orthoclase component (Table 1). The SEM-EDS results are thus less accurate in documenting NH_4^+ substitution in authigenic K-NH_4-feldspar.

In 7 of the 8 samples where authigenic K-NH_4-feldspar is present both as a microfracture filling and overgrowth cement, the concentration of NH_4^+ is systematically higher in the microfracture phase than in the cement. In individual cases this difference is as large as 26 mole % (Tab. 1). One special case was observed in the Oligocene Vedder Sand from the Fruitvale oil field. The authigenic K-NH_4-feldspar cement in this unit contains two petrographically distinguishable generations: an early pure K-feldspar and a later NH_4^+-bearing phase (Table 1).

The largest NH_4^+ value (80.5 mole % buddingtonite) was detected in a syntaxial overgrowth in a sample from the Antelope Formation (BAMA 1119.5, Table 3). A smaller concentration, but still approximately 50 mole %, is typical for authigenic K-NH_4-feldspar in samples from the Stevens Sands. This high value is in accord with the data of Compton et al. (1992), which show high nonexchangeable NH_4^+ concentrations in K-bearing minerals (e.g., K-feldspar, illite, I/S) in the surrounding Antelope shales. Similar high concentrations of NH_4^+ in K-NH_4-feldspar are known only from a mudstone interval in the Meade Peak Member of the Phosphoria Formation in SE Idaho, where up to 82 mole % NH_4^+ is present (Gulbrandsen 1974). Higher values up to the end-member composition of buddingtonite are typically found in oil-shale deposits (Loughnan et al. 1983) and hydrothermally altered andesitic lava flows (Erd et al. 1964), where ammonium contents in the bulk rocks were either originally high, or were raised by hydrothermal influxes.

K-NH_4-feldspar with low NH_4^+ values (i.e., < 30 mole %) is typical for samples from the shallow-marine Vedder Sands and the Pyramid Hill Sand Member, the marginal marine San Joaquin Formation, and the nonmarine Chanac Formation (Table 1, Fig. 1).

TIMING AND CONDITIONS OF AUTHIGENIC K-NH_4-FELDSPAR PRECIPITATION

At North Coles Levee authigenic K-NH_4-feldspar is present as microfracture fillings in detrital K-feldspar in zones pervasively cemented by carbonate. The petrographic relationships indicate clearly that the K-NH_4-feldspar crystallized prior to carbonate cementation. In sample NCL 2727.4 from the same locality, $\delta^{18}O$ analyses reveal that the dolomite cement formed at 28°C (Table 2; for more details see Boles and Ramseyer 1987, Schultz et al. 1989). Authigenic K-NH_4-feldspar thus appears able to crystallize at temperatures below 28°C. Similarly, a maximum crystallization temperature of 35°C is indicated by the present-day temperature of the authigenic K-NH_4-feldspar occurrence in the Round Mountain oil field (sample ROMO 568.5). In the remaining samples, maximum present-day temperatures are as high as 174°C, so it is not clear whether all the analyzed authigenic K-NH_4-feldspars precipitated at low temperatures. The petrographic and geochemical evidence that these feldspars precipitated within fractures formed by compaction forces constrains the possible depth of crystallization to at least several hundred meters below the sediment-water interface.

As well as providing the tightest temperature constraint, sample NCL 2727.4 from North Coles Levee also sheds light on the environment of authigenic K-NH_4-feldspar precipitation. The $\delta^{13}C$ value of the dolomite cement is positive, indicating that its CO_2 originated from bacterial decay of organic matter in the zone of methanogenesis (Table 2; Boles and Ramseyer 1987). Furthermore, the $^{87}Sr/^{86}Sr$ ratio of the cement is identical to the value for Late Miocene sea water determined on benthic foraminifera in the same strata at North Coles Levee (Table 2, Schultz et al. 1989). Taken collectively, these points of evidence show that authigenic K-NH_4-feldspar precipitated early in the diagenetic history, under anoxic conditions during methanogenesis (Coleman 1985; Curtis and Coleman 1986).

Other constraints on the relative timing of K-NH_4-feldspar precipitation may be drawn from the presence of diagenetic kaolinite in the southern San Joaquin Basin. The kaolinite crystallized during intermediate burial, preferentially in the oil zone of hydrocarbon reservoirs. It appears to have formed as a byproduct of the dissolution of detrital plagioclase by organic acids derived from oil (Boles 1992; Hayes and Boles 1992). Such kaolinite formed after the growth of authigenic K-NH_4-feldspar, thereby indicating an early-diagenetic timing of ammonium fixation. Recent fixation is excluded by the lack of a correlation between the nitrogen concentrations in modern gases in the Great Valley of California (Jenden et al. 1988) and the ammonium concentrations in the diagenetic K-NH_4-feldspars.

The above timing constraints can be quantified approximately by examining the present-day shut-in well temperatures in the North Coles Levee oil field (Boles and Ramseyer 1987; Schultz et al. 1989). The maximum formation temperature of 28°C obtained from sample NCL 2727.4 implies a maximum formation depth for the authigenic K-NH_4-feldspar of around 600 m. Geochronologic data for this field (Schultz et al. 1989) indicate that this maximum temperature would have been reached at the latest some 600,000 years after sediment deposition. These calculated depth-time values thus set stringent constraints on the conditions of ammonium fixation.

ORIGIN OF NH_4^+ IN AUTHIGENIC K-NH_4-FELDSPARS

The analytical results presented above demonstrate that authigenic K-NH_4-feldspar is common in the Tertiary basins studied and that the NH_4^+ concentration varies enormously on a basinwide scale. Some of this variation may be due to differences in the local environmental factors controlling fluid-mineral partitioning of ammonium, such as temperature, oxidation potential, competing reactions with other ammonium-bearing phases (e.g., illite, zeolites), surface-related kinetic effects, and so on. However, given the common siliciclastic nature of the sediments, any feasible variations in such factors are unlikely to have generated the large compositional differences observed between the authigenic K-NH_4-feldspars. For example, there is no systematic change in NH_4^+ content with depth, so temperature can be ruled out as a major governing parameter. Without

compositional data on the fluid phase from which the authigenic K-NH_4-feldspars precipitated, it is difficult to reconstruct the quantitative effect of these geochemical factors. Even so, the high NH_4^+ content of the authigenic K-NH_4-feldspars are remarkable in themselves, and raise the question of the ultimate origin of the ammonium. This problem is addressed in the following discussion.

One of the most striking features of Fig. 1 is the narrow range of K-NH_4 solid solution displayed by individual stratigraphic units (e.g., the Stevens and Vedder Sands), in contrast to the large basinwide variability. Only the Etchegoin Formation and the units from the uplifted area on the western margin display large internal variability. The extent of K-NH_4 solid solution in authigenic K-NH_4-feldspar is thus clearly related to the nature of the host stratigraphic unit, and this relationship in turn leads to several inferences regarding the origin of the incorporated ammonium.

The first possibility for consideration is that the NH_4^+ concentration in the K-NH_4-feldspar is directly controlled by the abundance of primary N-bearing detrital organic matter in the sediments. If this were the case, then a correlation would be expected between the present concentration of detrital organic matter in the sediments and the NH_4^+ content of the corresponding authigenic feldspars. Unfortunately, because only sandstones recovered from drill core have been examined in this study, neither the bulk analytical data nor the lithologic spectrum of samples is available to test this idea. Nevertheless, a close inspection of the mean NH_4^+ content of the authigenic feldspars reveals that the largest substitution occurs in the deeper-marine turbiditic Stevens Sands and its shallow-marine equivalent, the Santa Margarita Formation. Both units are spatially and temporally associated with the organic-rich Antelope Shale, which, at least on the western side of the basin, contains measurable amounts of inorganic fixed ammonium in K-aluminosilicates (Compton et al. 1992). Smaller extents of substitution, i.e., < 20 mole %, are found in the shallow-marine sands from the marginal-marine Pliocene San Joaquin Formation, the lowermost Miocene Pyramid Hill Sand Member, and the Oligocene Vedder Sands, as well as the nonmarine sands of the Chanac Formation. The available evidence is thus compatible with an internal, *in situ* origin of ammonium, but it is by no means conclusive.

The second possibility for the origin of the ammonium is a secondary, postdepositional external source such as the compactional and oil-bearing fluids that migrated through the basins under investigation. Insofar as fluid migration is influenced by lithologic properties, a correlation should be expected between primary lithology and NH_4^+ content of the authigenic feldspars. However, in contrast to the former hypothesis, no correlation should exist between the content of organic matter in the sandstones and the NH_4^+ concentration in the authigenic feldspar. Again the data are lacking to test this possibility. Although there is a vertical and lateral increase in NH_4^+ content in the Etchegoin–San Joaquin Formation (Fig. 1), these trends could arise either from a decrease in the primary organic matter in the sediments or from the longer transport distance from the underlying organic-rich sediments.

All of the calculated constraints on the temperature and depth of authigenic K-NH_4-feldspar precipitation are compatible with an external influx of ammonium. Evidence has been cited above that the pore fluid following K-NH_4-feldspar precipitation had maintained the same $^{87}Sr/^{86}Sr$ signature since sedimentation. This rules out influx of fluids from older or younger units but leaves open the possibility of lateral migration from contemporaneous units, for example from the Antelope shales. Petroleum cannot have been the source fluid at this time, however, for two reasons. First, at the low temperatures at which K-NH_4-feldspar precipitated, organic matter in the contemporaneous shales had not yet reached the maturity level for oil generation. Second, petroleum migration in the San Joaquin basin was accompanied by kaolinite formation, which according to the cement stratigraphy is clearly younger than the authigenic K-NH_4-feldspars (Boles 1992; Hayes and Boles 1992).

In summary, the evidence adduced supports both the hypothesis of an *in situ* source of ammonium and the hypothesis of lateral influx from time-equivalent shales. If only one of these two hypothetical sources actually existed, then bulk analyses of the content of organic matter in the sediments could perhaps discriminate between the two. On the other hand, it seems just as likely that both sources contributed to produce the observed distribution of authigenic K-NH_4-feldspar. Liberation of ammonium from bacterial decay of organic matter may thus have stabilized buddingtonite-rich feldspars, the excess ammonium then being transported as a dissolved component in aqueous fluids expelled laterally upon early-diagenetic mud compaction. Ammonium may have continued to be incorporated in authigenic K-NH_4-feldspar at sites along the fluid migration paths. The high observed NH_4^+ concentrations in authigenic K-NH_4-feldspar presumably require unusually high concentrations of ammonium in the diagenetic fluid phase to permit their stability. Therefore, while authigenic K-NH_4-feldspars in this interpretation appear to be fingerprints of the diagenesis of organic matter, rather than of petroleum migration, their occurrence is probably restricted to basins that are in any case rich in organic material, and hence are potential sources for petroleum generation.

CONCLUSIONS

(1) Authigenic K-NH_4-feldspar is common in sandstones from the southern San Joaquin and the Los Angeles Basins.

(2) Authigenic K-NH_4-feldspar is present in trace amounts preferentially as a microfracture filling in detrital K-feldspar grains and in a few cases also as an overgrowth cement. In samples where authigenic K-NH_4-feldspar is present as both a microfracture filling and overgrowth cement, the microfracture phase is systematically richer in NH_4^+ than the overgrowth.

(3) The observed NH_4^+ concentrations vary between 0 and 80 mole % buddingtonite component.

(4) High concentrations of NH_4^+ in authigenic K-NH_4-feldspar are common for turbiditic sandstones, whereas low concentrations are found in shallow, marginal-marine and nonmarine sandstones.

(5) Authigenic K-NH_4-feldspar is an early-diagenetic phase, formed below 28°C under anoxic conditions in the zone of methanogenesis before oil migration.

(6) The source of ammonium is bacterial decay of organic matter in shales and/or sandstones.

ACKNOWLEDGMENTS

This research was funded by the Swiss National Science Foundation (Grants No. 20-30854.91 K.R. and No. 21-26579.89 L.D.) and the National Science Foundation (NSF 17013, Boles). We thank S. Olaussen, O. Walderhaug and S. Morad for their constructive and thorough reviews. Samples were provided by the California Well Repository, ARCO, Texaco, and Tenneco.

REFERENCES

Armbruster, T., 1985, Ar, N_2, and CO_2 in the structural cavities of cordierite, an optical and X-ray single-crystal study: Physics and Chemistry of Minerals, v. 12, p. 233–245.

Bartow, A.J., and McDougall, K., 1984, Tertiary stratigraphy of the southeastern San Joaquin Valley, California: United States Geological Survey Bulletin 1529-J, p. 1–41.

Bent, J.V., 1985, Provenance of upper Oligocene–middle Miocene sandstones of the San Joaquin basin, *in* Graham, S.A., ed., Geology of the Temblor Formation, Western San Joaquin Basin: SEPM Pacific Section, Book 44, p. 97–120.

Berner, R.A., 1980, Early Diagenesis, A Theoretical Approach: Princeton Series in Geochemistry, Princeton University Press, Princeton, New Jersey, 241 p.

Boles, J.R., 1992, Evidence for oil-derived organic acids in reservoirs, *in* Kharaka, Y.K., and Maest, A.S., eds., Water-rock interaction: Proceedings of the 7th International Symposium on Water-Rock Interaction, Park City, Utah, USA, p. 311–314.

Boles, J.R., and Ramseyer, K., 1986, Mixed-layer illite/smectite minerals in Tertiary sandstones and shales, San Joaquin basin, California: Clays and Clay Minerals, v. 34, p. 115–124.

Boles, J.R., and Ramseyer, K., 1987, Diagenetic carbonate in Miocene sandstone reservoir, San Joaquin basin, California: American Association of Petroleum Geologists Bulletin, v. 71, p. 1475–1487.

Callaway, D.C., 1971, Petroleum potential of San Joaquin basin, California, *in* Cram, I.H., ed., Future Petroleum Provinces of the United States—Their Geology and Potential: American Association of Petroleum Geologists Memoir 15, p. 239–253.

COLEMAN, M.L., 1985, Geochemistry of diagenetic non-silicate minerals: kinetic considerations: Royal Society (London) Transactions, v. A315, p. 39–56.

COMPTON, J.S., WILLIAMS, L.B., AND FERRELL, R.E., JR., 1992, Mineralization of organogenic ammonium in the Monterey Formation, Santa Maria and San Joaquin basins, California, USA: Geochimica et Cosmochimica Acta, v. 56, p. 1979–1991.

CURTIS, C.D., 1978, Possible links between sandstone diagenesis and depth-related geochemical reactions occurring in enclosing mudstones: Geological Society of London Journal, v. 135, p. 107–117.

CURTIS, C.D., AND COLEMAN, M.L., 1986, Controls on the precipitation of early diagenetic calcite, dolomite, and siderite concretions in complex depositional sequences: SEPM Special Publication 38, p. 23–34.

DANIELS, E.J., AND ALTANER, S.P., 1990, Clay mineral authigenesis in coal and shale from the Anthracite region, Pennsylvania: American Mineralogist, v. 75, p. 825–839.

ERD, R.C., WHITE, D.E., FAHEY, J.J, AND LEE, D.E., 1964, Buddingtonite, an ammonium feldspar with zeolitic water: American Mineralogist, v. 49, p. 831–850.

FERRELL, R.E., AND WILLIAMS, L.B., 1991, Ammonium fixation during clay mineral diagenesis and hydrocarbon maturation: Clay Minerals Society 28th Annual Meeting, Houston, Texas, p. 49.

FRIEDMAN, I., AND O'NEIL, J.R., 1977, Compilation of stable isotope fractionation factors of geochemical interests: United States Geological Survey Professional Paper 440-KK, 12 p.

FRITZ, P., AND SMITH, D.C., 1970, The isotopic composition of secondary dolomites: Geochimica et Cosmochimica Acta, v. 34, p. 1161–1173.

FROELICH, P.N., KLINKHAMMER, G.P., BENDER, M.L., LUEDTKE, N.A., HEATH, G.R., CULLEN, D., DAUPHIN, P., HAMMOND, D., HARTMAN, B., AND MAYNARD, V., 1979, Early oxidation of organic matter in pelagic sediments of the eastern equatorial Atlantic: suboxic diagenesis: Geochimica et Cosmochimica Acta, v. 43, p. 1075–1090.

GRAHAM, S.A., AND WILLIAMS, L.A., 1985, Tectonic, depositional, and diagenetic history of Monterey Formation (Miocene), Central San Joaquin basin, California: American Association of Petroleum Geologists Bulletin, v. 69, p. 385–411.

GULBRANDSEN, R.A., 1974, Buddingtonite, ammonium feldspar, in the Phosphoria Formation, Southeastern Idaho: United States Geological Survey Journal of Research, v. 2, p. 693–697.

HALLAM, M., AND EUGSTER, P., 1976, Ammonium silicate stability relations: Contributions to Mineralogy and Petrology, v. 57, p. 227–244.

HAQ, B.U., HARDENBOL, J., AND VAIL, P.R., 1987, Chronology of fluctuating sea levels since Triassic: Science, v. 235, p. 1156–1167.

HAYES, M.J., AND BOLES, J.R., 1992, Volumetric relations between dissolved plagioclase and kaolinite in sandstones: implications for aluminum mass transfer in the San Joaquin Basin, California: SEPM Special Publication 47, p. 111–123.

JENDEN, P.D., KAPLAN, R.I., POREDA, R.J., AND CRAIG, H., 1988, Origin of nitrogen-rich natural gases in the California Great Valley: evidence from helium, carbon and nitrogen isotope ratios: Geochimica et Cosmochimica Acta v. 52, p. 851–861.

KASTNER, M., AND SIEVER, R., 1979, Low temperature feldspars in sedimentary rocks: American Journal of Science, v. 279, p. 435–479.

KRUMBEIN, W.E., 1983, Microbial Geochemistry: Oxford, Blackwell Scientific Publications, 330 p.

LOUGHNAN, F.C., ROBERTS, I.V., AND LINDNER, A.W., 1983, Buddingtonite (NH_4-feldspar) in the Condor oilshale deposit, Queensland, Australia: Mineralogical Magazine, v. 47, p. 327–334.

MARSHALL, D.J., 1988, Cathodoluminescence of Geologic Materials: Boston, Unwin Hyman, 146 p.

MOXON, I.W., 1988, Sequence stratigraphy of the Great Valley basin in the context of convergent margin tectonics, *in* Graham, S.A., ed., Studies of the Geology of the San Joaquin Basin: SEPM Pacific Section, Book 60, p. 3–28.

POUCHOU, J.L., AND PICHOIR, F., 1984, Un nouveau modèle de calcul pour la microanalyse quantitative par spectrométrie de rayons X. La Recherche Aèrospatiale, v. 3, p. 167–192.

RAMSEYER, K., BOLES, J.R., AND LICHTNER, P.C., 1992, Mechanism of plagioclase albitization: Journal of Sedimentary Petrology, v. 62, p. 349–356.

RAMSEYER, K., FISCHER, J., MATTER, A., EBERHARDT, P., AND GEISS, J., 1989, A cathodoluminescence microscope for low intensity luminescence: Journal of Sedimentary Petrology, v. 59, p. 519–622.

SCHULTZ, J.L., BOLES, J.R., AND TILTON, G.R., 1989, Tracking calcium in the San Joaquin basin, California: a strontium isotopic study of carbonate cements at North Coles Levee: Geochimica et Cosmochimica Acta, v. 53, p. 1991–1999.

WEBB, G.W., 1981, Stevens and earlier Miocene turbidite sandstones, southern San Joaquin Valley, California: American Association of Petroleum Geologists Bulletin, v. 65, p. 438–465.

WILLIAMS, L.B., FERRELL, R.E., CHINN, E.W., AND SASSEN, R., 1989, Fixed-ammonium in clays associated with crude oils: Applied Geochemistry, v. 4, p. 605–616.

WILLIAMS, L.B., WILCOXON, B.R., FERRELL, R.E., AND SASSEN, R., 1992, Diagenesis of ammonium during hydrocarbon maturation and migration, Wilcox Group, Louisiana, U.S.A.: Applied Geochemistry, v. 7, p. 123–134.

WOOD, J.R., AND BOLES, J.R., 1990, Evidence for episodic cementation and diagenetic recording of seismic pumping events, North Coles Levee, California, U.S.A.: Applied Geochemistry, v. 6, p. 509–521.

Manuscript received 1 March 1993; accepted 14 April 1993.